Vorticity dynamics, drift wave turbulence, and zonal flows: a look back and a look ahead

To cite this article: P H Diamond *et al* 2011 *Plasma Phys. Control. Fusion* **53** 124001

Plasma Phys. Control. Fusion **53** (2011) 124001 (23pp) doi:10.1088/0741-3335/53/12/124001

Vorticity dynamics, drift wave turbulence, and zonal flows: a look back and a look ahead

P H Diamond[1,2], **A Hasegawa**[3] **and K Mima**[4]

[1] WCI Center for Fusion Theory, NFRI, Korea
[2] CMTFO and CASS, UCSD, USA
[3] Osaka University, Japan
[4] The Graduate School for the Creation of New Photonics Industries and ILE, Osaka University, Japan

Received 20 July 2011, in final form 5 September 2011
Published 14 November 2011
Online at stacks.iop.org/PPCF/53/124001

Abstract
This paper surveys the basic ideas and results on fundamental models of drift wave turbulence, the formation of zonal flows, shear suppression of turbulence and transport, coupled drift wave and zonal flow dynamics and application to transport bifurcations and transitions. Application to vortex dynamics and zonal flow phenomena in EMHD systems are discussed, as well. These are relevant to aspects of ICF and laser plasma physics. Throughout, an effort is made to focus on fundamental physics ideas.

(Some figures in this article are in colour only in the electronic version)

1. Introduction

Inhomogeneity of plasma profiles in magnetically confined plasmas is responsible for the generation of various instabilities that may lead to turbulent plasma states. The study of heat and particle confinement of plasmas in the presence of such turbulence is a fundamental issue for the success of controlled thermonuclear fusion. We address this issue in this paper. In the first part, we present the historical developments of the theory of strong electrostatic turbulence of magnetically confined plasmas and of the generation of azimuthal zonal flows. The model equation (the Hasegawa–Mima equation [5]) that includes plasma density inhomogeneity, nonlinear convection of plasma vortices and Boltzmann electrons has two quadratic independent globally conserved quantities in the inviscid limit, energy and potential enstrophy. This fact indicates inverse cascade of turbulent energy spectra and the condensation of the spectrum to form a zonal flow in the azimuthal direction [10, 11]. Supporting simulation results are discussed.

The second part of the paper reviews the essential elements of the theory of drift wave–zonal flow turbulence [9]. The dynamics of zonal flow generation by potential vorticity (PV) or polarization charge transport [28] and the shearing feedback of zonal flows on the underlying microturbulence are discussed. We show that PV transport or mixing is fundamental to zonal

flow formation. Shear decorrelation [30] physics is elucidated. Special attention is focused on the self-consistent feedback loop system—i.e. the predator–prey model [35, 37]—formed by the turbulence and flow shears. Simulation results [36] supporting the predator–prey model are reviewed. The relevance of these ideas to the ongoing quest to understand the $L \rightarrow H$ transition and multi-predator prey models [37] relevant to the $L \rightarrow H$ transition are discussed.

The third part deals with the application to electron magnetohydrodynamics (EMHD). EMHD [64] plays important roles in laser plasmas [65–70], magnetic field reconnection plasmas [71–77] and space and astronomical plasma phenomena [78, 79] when the space and time scales are much shorter than the ion scales. The electromagnetic fluctuations with frequencies much lower than the electron plasma frequency have structures like whistler waves. The turbulence of such electromagnetic fluctuations are so-called whistler turbulence. Examples of whistler turbulence are the turbulence predicted by the models of gamma ray burst [78, 79] and by the models for relativistic electron beam transport in plasmas [68, 69]. The whistler turbulence also plays important roles in collisionless magnetic reconnection in solar flare and magnetosphere [71–77].

The rest of the paper is organized as follows. Section 2 deals with the formulation of the basic models and the basic aspects of zonal flow formation. Section 3 continues the discussion of zonal flow physics and formation, addresses shear suppression and describes the coupled dynamics of drift waves and zonal flows. Section 4 presents the application to EMHD vortices and structures. It also addresses applications of the ideas to problems in ICF and laser plasma physics. The last part of the paper is a brief conclusion and outlook.

2. Drift wave vortex models and zonal flows

2.1. Background

The study of plasma turbulence started almost immediately following the development of plasma physics, since plasma was recognized as intrinsically nonlinear. In the early stages, the weak turbulence theory based on perturbation analysis was popular, but starting in the late 1970s, when diagnosis based on electromagnetic wave scattering revealed strong turbulence property, attention to the theory of strong plasma turbulence increased. Hasegawa and Mima derived a model equation that describes the strong electrostatic turbulence based on the nonlinear convection of ion vortices that accompanies plasma density fluctuations. The equation demonstrates an existence of conservation of (potential) enstrophy (squared vorticity) in addition to energy. Analogy of this property to the two-dimensional Navier–Stokes equation led the authors to predict an inverse spectral cascade and formation of self-organization of the turbulence. In the 1980s, Hasegawa together with Wakatani, extended the Hasegawa–Mima equation to include driving terms of the turbulence based on resistivity and magnetic field curvature and demonstrated the inverse cascade that leads to the formation of the azimuthal zonal flow. They further predicted that the zonal flow could inhibit turbulent radial loss of the plasmas. Anomalous plasma loss due to turbulence has been the major concern in plasma confinement with a magnetic field, however, the prediction by Hasegawa and Wakatani proved a hope that plasma can be confined by its own turbulent property. In this section, we also add some recent simulation results that support such possibilities.

2.2. Derivation of the Hasegawa–Mima equation

When Mima was visiting Hasegawa at Bell Laboratories in 1976, we were introduced to very interesting laser scattering data by Slusher and Surko [1] obtained from density fluctuations

of the drift wave frequency range of a Princeton tokamak. The data, in agreement with those obtained by Mazzucato [2] by microwave scattering, showed a very broad frequency spectrum whose width is wider than the expected drift frequency itself. Hasegawa and Mima were intrigued by the data and immediately constructed a theory of drift wave turbulence that may account for this unexpected data. In response, to answer criticism that the broad spectra might have been due to the path averaging of the scattering date, Slusher and Surko [3] later performed a pin point scattering experiment by means of two lasers and demonstrated the validly of the earlier data.

We recognized that in order to account for the density fluctuation observed by those data, one needs to take into account compressible ion flow. Since $E \times B$ drift is incompressible, we recognized the importance of the polarization drift, which is intrinsically nonlinear because of the convective electric field. We then realized that this nonlinear polarization drift could best be recognized as nonlinear. The ion vorticity Ω due to the $E \times B$ drift can describe the Laplacian of the electrostatic potential ϕ,

$$\Omega = (\nabla \times \boldsymbol{v}_\perp) \cdot \hat{z} = \nabla \times \left(\frac{-\nabla\phi \times \hat{z}}{B_0} \right) \cdot \hat{z} = \frac{\nabla_\perp^2 \phi}{B_0}. \tag{1}$$

Here, B_0 is the flux density of the ambient magnetic field and $\nabla_\perp^2$ is the Laplacian operator in the direction perpendicular to the magnetic field. The equation of ion vorticity can be constructed by taking a curl of the ion equation of motion in the direction normal to the ambient magnetic field. If the pressure and density gradients are parallel, the equation reads

$$\frac{\mathrm{d}}{\mathrm{d}t}(\Omega + \omega_{\mathrm{ci}}) + (\Omega + \omega_{\mathrm{ci}}) \nabla \cdot \boldsymbol{v}_\perp = 0. \tag{2}$$

Here ω_{ci} is the ion cyclotron frequency. The compressible ion flow is related to the ion density fluctuation, n, through the continuity equation

$$\nabla \cdot \boldsymbol{v}_\perp = -\frac{\mathrm{d}}{\mathrm{d}t} \ln n = -\frac{\mathrm{d}}{\mathrm{d}t} \left(\ln n_0 + \frac{e\phi}{T_{\mathrm{e}}} \right). \tag{3}$$

Here, the quasi-neutrality condition relates the ion density fluctuation to that of electrons, which will obey the Boltzmann equilibrium in this frequency range due to their inertia-less motions along the magnetic field. At this point the reader should recognize that even if we treat ions in the two-dimensional plane normal to the direction of the magnetic field, we allow electron dynamics in three dimensions here.

From equations (2) and (3), we can construct the equation for ion vorticity for its compressible flow,

$$\frac{\mathrm{d}}{\mathrm{d}t} \left(\ln \frac{\omega_{\mathrm{ci}}}{n_0} + \frac{\Omega}{\omega_{\mathrm{ci}}} - \frac{e\phi}{T_{\mathrm{e}}} \right) = \left(\frac{\partial}{\partial t} - \frac{\nabla\phi \times \hat{z}}{B_0} \cdot \nabla \right) \left(\ln \frac{\omega_{\mathrm{ci}}}{n_0} + \frac{\Omega}{\omega_{\mathrm{ci}}} - \frac{e\phi}{T_{\mathrm{e}}} \right). \tag{4}$$

Equation (4) shows that the time evolution of vorticity and potential becomes nonlinear due to the nonlinear convection of the ion vorticity, as is expected, while the nonlinear convection of the potential does not contribute to the nonlinear response. Furthermore, if the spatial scale is on the order of the ion gyro radius at the electron temperature, which is the case of drift wave type fluctuations, the space-time evolution of the potential field becomes fully nonlinear if the normalized potential field, $e\phi/T_{\mathrm{e}}$ becomes of the order of the ratio of drift wave frequency to the ion cyclotron frequency, which is very small.

Thus, for these space–time scales, the evolution of the potential field becomes fully nonlinear and is given by

$$\frac{\partial}{\partial t}(\nabla_\perp^2 \phi - \phi) - \nabla\phi \times \hat{z} \cdot \nabla \left[\nabla_\perp^2 \phi - \frac{1}{\epsilon} \ln \left(\frac{n_0}{\omega_{\mathrm{ci}}} \right) \right] = 0. \tag{5}$$

Here the small parameter ϵ represents the normalized amplitude as well as the time as shown below,

$$\epsilon\omega_{ci}t \equiv t, \qquad x/\rho_s \equiv x, \qquad e\phi/T_e \equiv \epsilon\phi, \qquad \text{where } \rho_s = \sqrt{T_e/m_i}/\omega_{ci}. \tag{6}$$

Equation (5) describes a fundamental property of electrostatic plasma turbulence in the drift wave frequency range in the absence of dissipations and is often referred to as the Hasegawa–Mima equation [5].

2.3. Conservation laws, inverse cascades in the kinetic and hydrodynamic regimes

The model equation (5) that describes the drift wave turbulence demonstrates that the drift wave becomes fully nonlinear even at a very low fluctuation level. In this section, we describe general properties of drift wave turbulence in hydrodynamic as well as in kinetic regimes based on this model equation.

2.3.1. Conservation laws. Equation (5) has interesting conservation laws and consequences. First it has energy conservation, which can be constructed by multiplying it with ϕ and integrating over the volume,

$$\frac{\partial W}{\partial t} \equiv \frac{\partial}{\partial t}\int [(\nabla_\perp \phi)^2 + \phi^2]\,\mathrm{d}V = 0. \tag{7}$$

Thus the sum of the kinetic and potential energies is conserved. The interesting part of the conservation law is that there exists additional conservation. The secondary conservation is the sum of the enstrophy, the squared vorticity, and the kinetic energy, sometimes called the potential enstrophy,

$$\frac{\partial U}{\partial t} \equiv \frac{\partial}{\partial t}\int [(\nabla_\perp \phi)^2 + (\nabla_\perp^2 \phi)^2]\,\mathrm{d}V = 0. \tag{8}$$

The presence of conservation of the enstrophy in addition to the energy has been familiar in two-dimensional hydrodynamics and the interesting nature of its turbulence has been studied.

2.3.2. Boltzmann statistics. In the absence of dissipation, the Boltzmann statistics that are obtained by minimizing the entropy in such a system have a strange character because of the additional constraint that comes from enstrophy conservation: the distribution function f that maximizes entropy with constraints of conservation of energy and enstrophy should read,

$$\delta\left(\int f \ln f\,\mathrm{d}V - \lambda_1 W - \lambda_2 U\right) = 0. \tag{9}$$

Here λs are Lagrange multipliers, and the resultant distribution function is given by

$$f \sim \exp(-\lambda_1 W - \lambda_2 U). \tag{10}$$

In the wave number space, since $U_k = k^2 W_k$, the average energy per mode becomes

$$\langle W_k \rangle = \frac{1}{\lambda_1 + k^2 \lambda_2}. \tag{11}$$

As pointed out by Onsager [6], this result not only violates the equipartition law but also could result in a negative temperature if the product of λ_1 and λ_2 is negative, thus modal statistics can be strange, indicating consequences that may lead to unexpected states.

2.3.3. Self-organized state in the hydrodynamic regime. In the presence of dissipation, turbulence described by the Hasegawa–Mima equation may lead to a dual cascade of the spectrum as pointed out by Kraichnan for two-dimensional Navier–Stokes turbulence. The inertial range Kolmogorov spectra [7] can be defined dually, one for energy and the other for enstrophy. Since the enstrophy spectrum has larger k dependence, it tends to get dissipated by viscosity preferentially and as a result the energy spectrum cascades to small wavenumbers and condensates to a minimum wave number that the system allows. This is a process of self-organization of turbulence. The self-organized state can simply be described by variation of minimizing the enstrophy with the constraint of constant energy,

$$\delta(U - \lambda W) = 0. \tag{12}$$

With the help of the definition of the energy and the enstrophy in equations (7) and (8), equation (12) gives the eigenvalue equation for ϕ,

$$\nabla^2\phi + \lambda\phi = 0. \tag{13}$$

This may be solved for a given boundary condition and the smallest eigenvalue gives the self-organized state.

2.3.4. Weak turbulence theory. If the normalized amplitude of the wave is much smaller than the ratio of the drift wave frequency to the ion cyclotron frequency, the nonlinear term in the Hasegawa–Mima equation may be treated as perturbation and the evolution of the turbulent spectrum may be studied using the weak turbulence theory. We take three waves with wave numbers $\boldsymbol{k}_1$, $\boldsymbol{k}_2$ and $\boldsymbol{k}_3$, such that

$$k_1^2 \leqslant k_2^2 \leqslant k_3^2. \tag{14}$$

The linearized Hasegawa–Mima equation gives the drift wave frequency given by

$$\omega_{\boldsymbol{k}} = \frac{\boldsymbol{k} \times \hat{\boldsymbol{z}} \cdot \nabla \ln(\boldsymbol{n}_0/\omega_{\mathrm{ci}})}{\epsilon(1 + k^2)} \tag{15}$$

and the nonlinear term can be treated as a perturbation to produce coupling of the three waves [11]. In the three wave couplings, the number of wave quanta defined by

$$N_p = (1 + k_p^2)|\phi_p|^2/|k_q^2 - k_r^2|, \ k_p^2 \neq k_r^2 \tag{16}$$

is conserved so that

$$N_3 - N_1 = \text{const.}, \qquad N_1 + N_2 = \text{const.}, \qquad N_2 + N_3 = \text{const.} \tag{17}$$

This result shows that a loss of one quantum of the wave with wave number k_2 appears as a gain in one quantum of the wave with the wave numbers given by k_1 or k_3. This indicates a dual cascade of energy to smaller and larger wave numbers. A clearer picture that is consistent with the well-known weak turbulence result can be obtained by requiring resonant three wave interactions such that the wave matching condition is satisfied. This is possible in a small wave number region such that,

$$k_q^2 - k_r^2 = k_{qy}/\omega_q - k_{ry}/\omega_r = \omega_p M, \tag{18}$$

where k_y is the wave number in the direction of $\hat{z} \times \nabla \ln n_0$ and

$$M \equiv \frac{\omega_p(k_{ry} - k_{qy}) + \omega_q(k_{py} - k_{ry}) + \omega_r(k_{qy} - k_{py})}{3\omega_p\omega_q\omega_r}. \tag{19}$$

In this regime, the wave energy decays into smaller frequencies since the wave quanta defined by

$$N_k = W_k/\hbar\omega_k \tag{20}$$

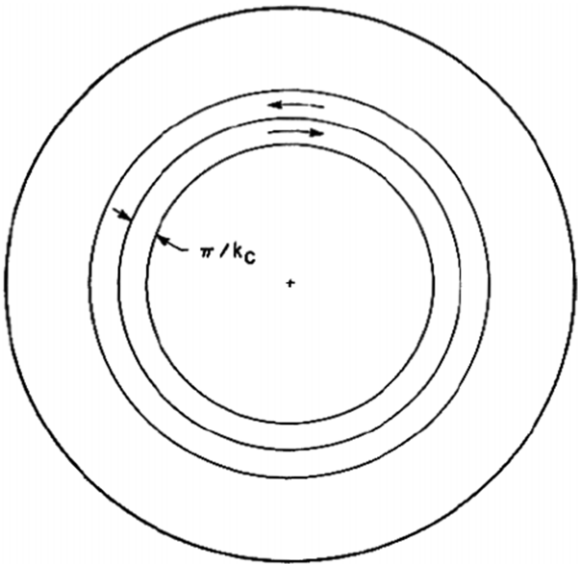

Figure 1. Zonal flow pattern predicted from the weak turbulence theory.

is conserved. Since the drift wave frequency is proportional to k_y this result indicates that the wave energy decays to that with smaller k_y keeping k_x more or less constant at $1/\rho_s(\equiv k_c)$. In a cylindrical plasma, this indicates that the wave energy cascades to a mode having zero azimuthal wave numbers as shown in figure 1, with radial wave number being kept at k_c. The theory presented by Hasegawa *et al* [11] is the first prediction of the formation of the zonal flow.

2.4. Introduction of the Hasegawa–Wakatani model and prediction of the zonal flow in the hydrodynamic regime

If the free energy source is large enough, the level of wave amplitude will approach the ratio of the drift wave frequency to the ion cyclotron frequency. Then the drift wave becomes fully nonlinear as indicated by the Hasegawa–Mima equation. This may be the case when the wave is generated by a combination of magnetic field curvature and pressure gradient. Hasegawa and Wakatani [12] developed a model that describes evolution of the electrostatic potential ϕ and the density fluctuation n for such a case. They included electron resistivity and ion viscosity, which are responsible for the excitation of the curvature driven instability and dissipation of the excited turbulence. In a cylindrical geometry the equation of vorticity reads

$$\frac{\rho_s^2}{a^2}\frac{\mathrm{d}}{\mathrm{d}t}\nabla_\perp^2\phi = (\nabla \ln n \times \nabla\Lambda)\cdot\hat{z} + \frac{\omega_{ce}}{\nu_{ei}}\left(\frac{a}{R}\right)^2\nabla_\parallel^2(\ln n - \phi) + \frac{\mu}{\omega_{ci}a^2}\nabla_\perp^4\phi. \tag{21}$$

Here $\nabla\Lambda$ represents the curvature of the toroidal magnetic field, ω_{ce} and ν_{ei} are the electron cyclotron frequency and electron–ion collision frequency, a and R are the minor and major radius of the toroidal container and μ represents the ion viscosity. The equation of continuity is also modified due to the curvature and reads

$$\frac{\mathrm{d}}{\mathrm{d}t}\ln n = (\nabla \ln n \times \nabla\Lambda)\cdot\hat{z} + \frac{\omega_{ce}}{\nu_{ei}}\left(\frac{a}{R}\right)^2\nabla_\parallel^2(\ln n - \phi). \tag{22}$$

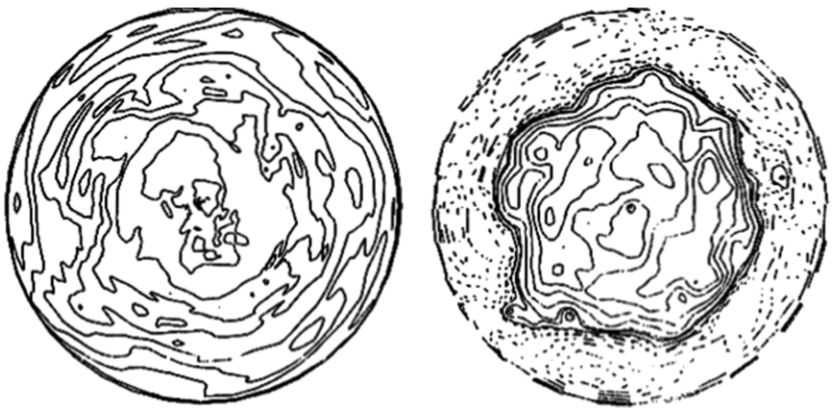

Figure 2. Equipotential contour of simulation results obtained from equations (21) and (22). The solid (dotted) lines are for positive (negative) equipotentials. It is clear that the curvature driven plasma turbulence produces a self-organized state in which a global equipotential has a $\phi = 0$ closed surface near the outer edge of the plasma.

Equations (21) and (22) form a closed set of nonlinear equations that describe the evolution of the potential and density fields. Even in the presence of the curvature terms, it can be shown that in the inviscid limit, the total energy and potential enstrophy are conserved;

$$W = \frac{1}{2}\int \mathrm{d}V \left[(\ln n)^2 + \frac{\rho_s^2}{a^2}(\nabla_\perp \phi)^2\right] \tag{23}$$

and

$$U = \frac{1}{2}\int \mathrm{d}V \left[\frac{\rho_s^2}{a^2}\nabla_\perp^2 \phi - \ln n\right]^2. \tag{24}$$

The conservation of W and U indicates the existence of inverse cascade of the energy spectrum as discussed earlier. In the case of toroidal plasma, in addition to these two conservations, the total angular momentum in the poloidal direction (which should be zero) should also be conserved. Thus the self-organized state should be obtained by minimizing the potential enstrophy, (23) with constraints of conservation of energy (24) as well as the total toroidal angular momentum. This will lead to a self-organized structure in which the minimum eigenvalue has a node between the center and the wall. As a result, at self-organization, the radial electric field reverses its sign at some radial position. The minimization of the potential enstrophy with these constraints will lead to the generation of a global azimuthal flow of the plasma that will have a shear. Equations (21) and (22) are numerically solved to trace the evolution of the turbulence spectrum excited by the magnetic field curvature. Results of the simulation are shown in figure 2. Here the left figure is the initial potential profile (stream function), which is randomly given, and the right figure shows the potential profile at a final time. Here the dotted lines show negative equipotential lines. One can see in this figure that the self-organized state produces an equipotential line that has a closed node at some outer radial position indicating the formation of a global azimuthal shear flow.

In figure 3 we show the evolution of the radial potential profile in the simulation. Here the solid line indicates the theoretically predicted self-organized state based on the minimization of the potential enstrophy with constraints of both the total energy and the global angular momentum. This figure shows clearly that the self-organized state produces a global radial electric field that reverses its sign. This electric field creates an $E \times B$ rotation of plasma

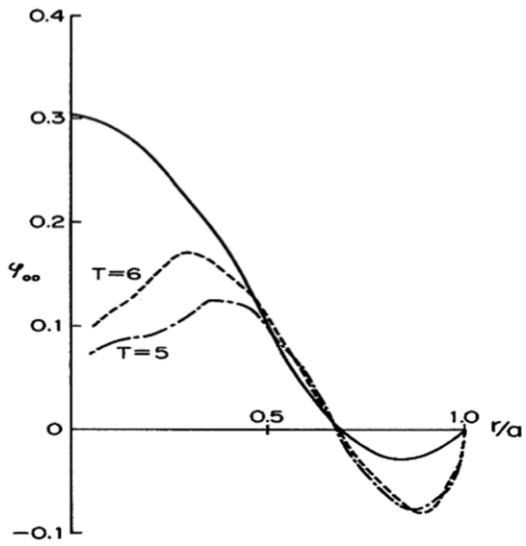

Figure 3. Temporal variations of the radial profile of the axis symmetric potential profile are shown for different time. The solid line is the theoretically predicted potential profile obtained from the self-organization theory.

in the azimuthal direction that changes direction at some radius indicating a generation of an azimuthal shear flow. This we believe is the first observation of a zonal flow generation in turbulent plasma. The zonal flow structure is global rather than microscopic as indicated in the kinetic theory, figure 1. It may be due to the fact that the instability here is driven by global magnetic field curvature, which is hydrodynamic.

2.5. What are the effects of zonal flow on plasma transport?

Zonal flows have been observed to inhibit the transport of vortex eddies across the flows. One well-known example is the atmospheric dynamics of the planet Jupiter. As has been demonstrated by Hasegawa *et al* [11], the Hasegawa–Mima equation has a structure mathematically identical to that which describes the horizontal motion of planet atmosphere with gravity and gradient of the Coriolis force. On a planet surface, the latitudinal direction in which the Coriolis parameter varies corresponds to the radial direction in cylindrical plasma, the longitudinal direction corresponds to the azimuthal direction and the vertical direction to the axial direction. Figure 4 is the well-known picture of Jovian atmosphere.

Analogy of the mathematical structure of the model equation that describes the plasma turbulence in the magnetic field to that of the planetary atmospheric motion indicates that a similar turbulent dynamics may operate also in plasmas. The simulation result obtained by Hasegawa and Wakatani [12] in fact indicates that convection of the plasma vortices seems to be inhibited across the equipotential surface of $\phi = 0$. Since electrons are expected to move on the constant ϕ surface, if vortices cannot convect across this surface, zonal flows are expected to inhibit electron transport in the radial direction. This fact is indicative of a very interesting process in which the instability excited self-organized state of plasma may inhibit anomalous electron transport in the radial direction. This contradicts the previously known effect of plasma turbulence that predicts anomalous diffusion. In fact, the reduction of the transport in the presence of zonal flows is verified numerically in resistive pressure-gradient-driven

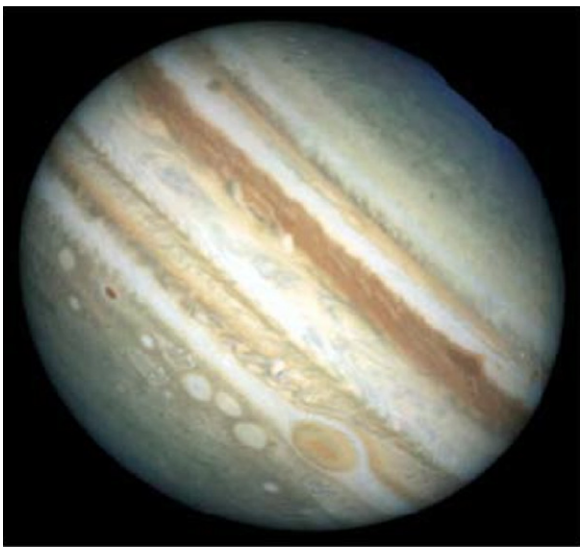

Figure 4. A profile of atmospheric motion on the Jovian surface. The existence of longitudinal zonal flows is clearly visible. The zonal flows are seen to inhibit the convection of atmospheric vortices in the latitudinal direction crossing the flow.

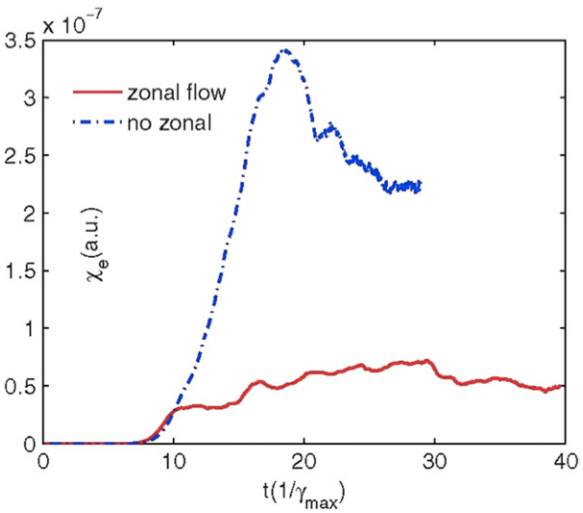

Figure 5. Simulation result obtained by Xiao *et al* (2010) [15]. The figure shows time evolution of electron heat transport. The solid line is the heat transport obtained in the simulation where self-generated zonal flow is present, while the dotted lines is the heat transport in which the zonal flows are artificially removed.

turbulence [13], ion temperature gradient turbulence [14], collisionless trapped electron mode turbulence [15], as well as other models. Figure 5 shows the reduction of electron heat conduction in the presence of zonal flows.

Although at present, the existence of zonal flows and their possible role in the reduction of anomalous transports have been confirmed in various experiments, theoretical studies on the

stability of the zonal flow and its influence on plasma transport are still actively being pursued. This is the subject of study presented in the next section.

3. Zonal flows and shear suppression in drift wave turbulence

In this section, we briefly summarize progress in the theory of zonal flows and velocity shear suppression of drift wave turbulence. The discussion consists of a review of basic zonal flow physics, the dynamics of shearing and its relation to zonal flow formation and the behavior of the dynamical system defined by the coupled flows and fluctuations. Some applications of the theory to problems of current interest are discussed. A zonal flow [9] is an $n = 0, m = 0$ potential fluctuation with finite k_r. Given their structure, zonal flows may be thought of as secondary (nonlinearly driven) modes of minimal inertia [10, 11] and minimal damping [16] which drive no transport. Zonal flows are thus natural repositories in which to safely retain energy released by gradient driven microturbulence.

While there are several approaches to explain zonal flow generation, including modulational calculations via the reductive perturbation method [17–20], the fundamental mechanism of zonal flow formation in a quasi-2D fluid or plasma is PV transport or mixing in a system with one direction of symmetry [21]. Kelvin's theorem underpins this idea. The physics of zonal flow formation was studied within the geophysical fluid dynamics community long before it became a hot topic in the plasma community. Indeed, the quasi-geostrophic equation was first derived by Charney in 1948 [22], and within a few years, Charney and Drazin [23] obtained a momentum conservation theorem which elucidated the nonlinear origin and dynamics of zonal flows. In a plasma, vorticity transport or mixing (i.e. $-\rho^2\langle\tilde{v}_r\nabla^2\tilde{\phi}\rangle$ where $\langle\ldots\rangle$ is an ensemble average) results from the breaking of guiding center ambipolarity and the structure of the gyrokinetic Poisson equation. The flux of vorticity or polarization charge is equivalent to a Reynolds force, as first shown by [24], i.e. $-\rho^2\langle\tilde{v}_{r,E}\nabla^2\tilde{\phi}\rangle = -\partial_r\langle\tilde{v}_{r,E}\tilde{v}_{\perp,E}\rangle$, where $\langle\tilde{v}_{r,E}\tilde{v}_{\theta,E}\rangle$ is the Reynolds stress. The first discussions of the relation between vorticity and wave momentum transport and zonal flow formation were by Diamond and Kim [25] and Diamond *et al* [26]. The fluctuation-driven Reynolds force in turn drives the flow. Vorticity transport depends critically upon the phase relation between $\tilde{v}_r$ and $\nabla^2\tilde{\phi}$. This cross-phase is determined by the microdynamics of the mixing process, i.e. in particular, the velocity shear. There are several viable candidate mixing processes, which include:

(i) direct dissipation, as by viscosity;
(ii) nonlinear coupling to small scale dissipation by the *forward* cascade of PV. This effectively replaces the molecular viscosity by an eddy viscosity;
(iii) Rossby or drift wave absorption at critical layers, where $\omega = k_x\langle V_x(y)\rangle$. This is essentially Landau resonance. Transport or mixing of the PV region requires the overlap of neighboring critical layers, leading to stochastization of flow streamlines. Stochastization of streamlines guarantees PV mixing much like stochastization of orbits leads to mixing of $\langle f\rangle$ in quasi-linear theory;
(iv) stochastic nonlinear wave-fluid element scattering, which is analogous to transport induced by nonlinear Landau damping.

Note that the more general concepts are stochasticity of streamlines and forward potential enstrophy cascade to small scale dissipation. Interestingly, when looking at the phenomenon of zonal flow self-organization from the standpoint of PV transport and mixing, it is the *forward enstrophy cascade* which is critical, and not the inverse energy cascade, as is conventionally mentioned! Finally, we observe that zonal flow acceleration is not necessarily a strongly nonlinear process. PV mixing can occur via wave absorption, and can be manifested in weak

turbulence, as an essentially quasi-linear process. In this regard, the reader should consult [27]. To relate the transport of PV to the energetics of an open system, it is useful to consider the simplest non-trivial system, namely that of Hasegawa and Wakatani [8]. This system has a conserved inviscid PV $q = n - \nabla^2\phi$. Note the obvious analogy between total PV and total charge (i.e. guiding center + polarization). Conservation of potential enstrophy $\langle q^2\rangle$ and some straight forward algebra yield the identity:

$$\langle \tilde{v}_r \nabla^2 \tilde{\phi}\rangle = \langle \tilde{v}_r \tilde{n}\rangle + (\partial_t \langle \tilde{q}^2\rangle + \partial_r \langle \tilde{v}_r \tilde{q}^2\rangle + D_0 \langle (\nabla \tilde{q})^2\rangle)/\langle q\rangle'. \tag{25}$$

Here $\langle \tilde{q}^2\rangle$ denotes fluctuation potential enstrophy, which was previously defined as U. This choice is motivated by the consideration that the potential vorticity q is conserved inviscidly and thus is the fundamental quantity in drift wave–zonal flow dynamics. The prime ($\langle ...\rangle'$) denotes the radial derivative and the Prandtl number $Pr \equiv \mu/D_0 = 1$ is assumed for simplicity, where D_0 is the particle diffusivity and μ is the viscosity. Equation (25) locks the Reynolds force to the driving flux and the local dissipation of fluctuation potential enstrophy (either by viscosity or local divergence/convergence of the turbulence spreading flux). Using large scale momentum balance, we can extend equation (25) to derive a zonal flow momentum theorem in the style of a Charney–Drazin theorem [23, 28], i.e.

$$\partial_t \{(\text{GWMD}) + \langle v_\theta\rangle\} = -\langle \tilde{v}_r \tilde{n}\rangle - \delta_t \langle \tilde{q}^2\rangle/\langle q\rangle' - \nu \langle v_\theta\rangle, \tag{26a}$$

$$\text{GWMD} = -\langle \tilde{q}^2\rangle/\langle q\rangle'. \tag{26b}$$

Here GWMD is the generalized wave momentum density (i.e. pseudomomentum) and $\delta_t \langle \tilde{q}^2\rangle/\langle q\rangle' \equiv (\partial_r \langle \tilde{v}_r \tilde{q}^2\rangle + D_0 \langle (\nabla \tilde{q})^2\rangle)/\langle q\rangle'$. Equation (26*a*) states that in the absence of a driving flux or a local potential enstrophy decrement, it is impossible to accelerate or maintain a zonal flow against drag with time stationary fluctuations. Physically, equation (26*a*) expresses the freezing in of quasi-particles into the flow, unless 'slippage' due to drive or dissipation is induced. Equation (26*a*) imposes a fundamental constraint on models of stationary zonal flows. These *must* be constructed using an explicit connection to the driving turbulent flux and fluctuation dissipation. Note that flow acceleration requires relative spatial separation of fluctuation drive and damping, as in drift wave eigenfunctions with an outgoing wave structure [25].

Of course, zonal flows are of great interest in fusion due to the fact that they can regulate turbulence by shearing. Figures 6 and 7 illustrate the effect of a self-generated shear flow on extended turbulent eddys. This effect was first explicitly stated and developed in the seminal paper by Biglari *et al* in 1990 [30]. Time stationary, coherent shearing has long been know to couple to diffusive scattering to yield an enhanced, hybrid decorrelation rate. This process was discussed by Kelvin, Taylor [24], Dupree [29], and then applied to tokamak shear flows by Biglari, Diamond and Terry. The hybrid decorrelation rate is

$$\frac{1}{\tau_{c,k}} = \left(\frac{k_\theta^2 \langle v_E\rangle'^2 D_\perp}{3}\right)^{1/3}. \tag{27}$$

When $k_\theta \langle v_E\rangle' \Delta_r > D_\perp/\Delta_r^2$, decorrelation will be enhanced relative to the rate for zero shear. Important corrections to the theory of shear decorrelation related to shaping and compression were noted by Hahm and Burrell [31]. Other, linear shearing effects include spatial resonance dispersion ($\omega - k_\parallel v_\parallel \to \omega - k_\parallel v_\parallel - k_\theta \langle v_E\rangle'(r - r_0)$) and differential response rotation. An important caveat is that modes can adjust to weaken the effects of externally prescribed shear [32]. Thus, there is a qualitative difference between the effects of self-consistent, energy conserving zonal shears and externally prescribed shears. Zonal shears are most effectively described by wave kinetics, based on eikonal theory [9, 33]. In wave kinetics, shear acts to tilt

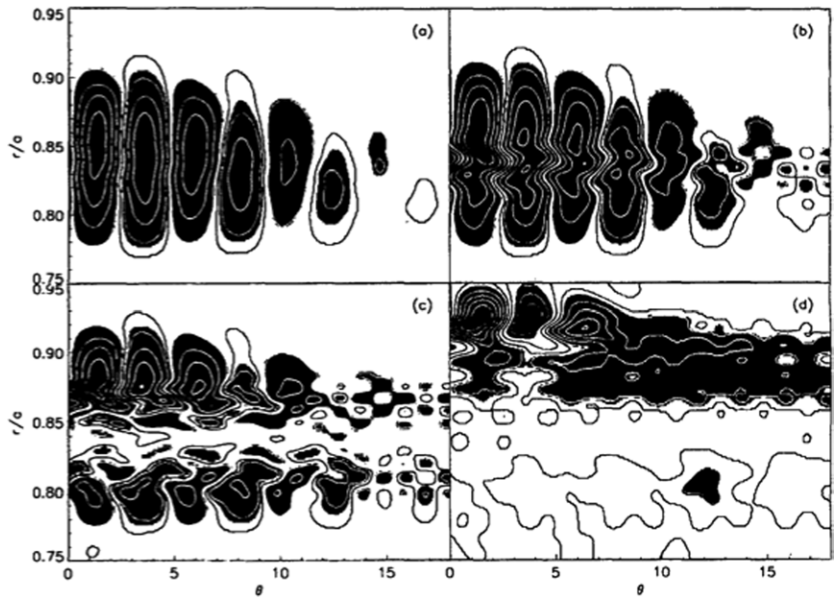

Figure 6. Flow effect on fluctuation. This figure, from [36], illustrates the effect of shearing on the fluctuation structure and scale.

and stretch vortices, thus increasing k_r. For a coherent shear, we have $k_r = k_r^{(0)} - k_\theta \langle v_E \rangle' \tau$ after a time duration τ, while for wave packet propagation in a complex shearing pattern, the wave packet undergoes induced diffusion in k_r, so $\langle \delta k_r^2 \rangle = D_k \tau$, where $D_k = \sum_q k_\theta^2 |\tilde{v}_E, q'|^2 \tau_{k,q}$. The physics of induced diffusion is a random walk of the wave packet k_r due to wave ray chaos, caused by overlap of resonances between zonal shear phase velocities and wave packet group velocity. Here $\tau_{k,q}$ is the correlation time of a wave packet $\boldsymbol{k}$ with zonal mode $\boldsymbol{q}$. The mean wave action (population) density equation thus becomes

$$\frac{\partial}{\partial t}\langle N \rangle - \frac{\partial}{\partial k_r} D_k \frac{\partial \langle N \rangle}{\partial k_r} = \gamma_k \langle N \rangle - \langle C\{N\} \rangle. \tag{28}$$

As a consequence, the effect of zonal flow shearing on wave energy is given by

$$\frac{\partial}{\partial t}\langle \epsilon \rangle = -\int \mathrm{d}\boldsymbol{k} v_{gr}(\boldsymbol{k}) D_k \frac{\partial \langle N \rangle}{\partial k_r} \tag{29}$$

so that for wave enstrophy density decreasing with k_r (i.e. $\mathrm{d}\langle \Omega \rangle / \mathrm{d}k_r < 0$), wave energy is damped. The fate of the energy is clear—it goes to the zonal flow via Reynolds work, as can be demonstrated by a modulational instability calculation [9, 34]. The bottom line, then, is that for zonal flows 'Reynolds work' and 'flow shearing' emerge as relabelings of one another, so that the energy budget always balances, intrinsically. This relation is the energy counterpart of the Charney–Drazin theorem for momentum [28] and of the proof of conservation of energy between waves (zonal modes) and particles (drift wave packets) in quasi-linear theory. In this light, the zonal flow damping mechanism emerges as critical to the self-regulation process, as it is a damping for the whole *system*. This follows from the structure of the predator–prey dynamics paradigm applicable to the drift wave–zonal flow interaction.

We have established that zonal flows regulate drift waves by shearing, while at the same time drift wave turbulence pumps the zonal flows. These two populations thus naturally form a self-regulating 'predator–prey' feedback loop. This loop is depicted in figure 8. The

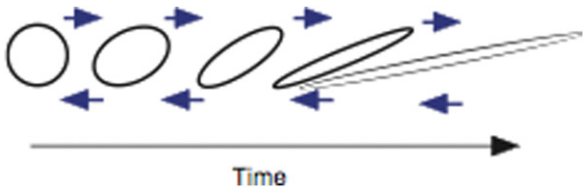

Figure 7. Stretching of eddy.

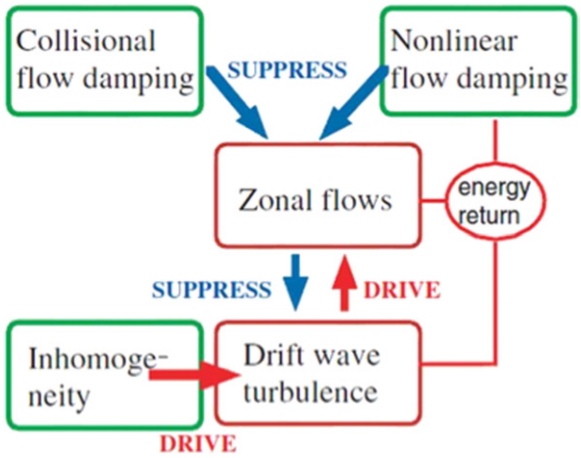

Figure 8. Predator–prey feedback loop structure [9] for the drift wave–zonal flow system, i.e. equations (30*a*) and (30*b*).

control parameters for this system are the sources (i.e. heat flux, etc) and the zonal flow damping. Interestingly, the predator–prey system reflects the underlying dual cascade of quasi-2D fluids. To see this, note that the prey equation for mean wave action density (related to wave potential enstrophy density) involves induced diffusion to high k_r, which is analogous to the forward enstrophy cascade. Likewise, the prey equation for the zonal flow energy describes the 'negative viscosity phenomenon' of zonal flow growth by wave Reynolds work and so is clearly analogous to the inverse energy cascade. We emphasize, however, that these two transfer processes are *not* local, as in the conventional cascade picture. The mean field predator–prey system may be reduced to a simple dynamical system,

$$\partial_t N = \gamma N - \alpha V^2 N - \Delta\omega N^2, \tag{30a}$$

$$\partial_t V^2 = \alpha N V^2 - \gamma_{\mathrm{d}} V^2 - \alpha_2 V^4. \tag{30b}$$

Here γ is the drift wave growth rate, $\Delta\omega$ is the turbulence nonlinear decorrelation rate, γ_{d} is the frictional zonal flow damping and α, α_2 are coefficients in the model, as given by equations (30*a*) and (30*b*) and discussed in [9]. This system exhibits multiple fixed points corresponding to no-flow and finite-flow states, respectively. These are discussed in [9, 35]. The roots and states are tabulated in figure 9. A value of the local growth, operationally set by the heat flux, sets the transition threshold, and the state transition occurs by a super-critical bifurcation in which a relaxation mode softens and goes unstable. Simple numerical experiments [36] have verified the predictions of this model (figure 10). In particular, these demonstrate the important role of zonal flow damping in regulating the drift wave–zonal flow system—see figure 11. This system, while conceptually instructive, is over-idealized. To

State	No flow	Flow ($\alpha_2 = 0$)	Flow ($\alpha_2 \neq 0$)
N (drift wave turbulence level)	$\frac{\gamma}{\Delta\omega}$	$\frac{\gamma_d}{\alpha}$	$\frac{\gamma_d + \alpha_2\gamma\alpha^{-1}}{\alpha + \Delta\omega\alpha_2\alpha^{-1}}$
V^2 (mean square flow)	0	$\frac{\gamma}{\alpha} - \frac{\Delta\omega\gamma_d}{\alpha^2}$	$\frac{\gamma - \Delta\omega\gamma_d\alpha^{-1}}{\alpha + \Delta\omega\alpha_2\alpha^{-1}}$
Drive/excitation mechanism	Linear growth	Linear growth	Linear growth Nonlinear damping of flow
Regulation/inhibition mechanism	Self-interaction of turbulence	Random shearing, self-interaction	Random shearing, self-interaction
Branching ratio $\frac{V^2}{N}$	0	$\frac{\gamma - \Delta\omega\gamma_d\alpha^{-1}}{\gamma_d}$	$\frac{\gamma - \Delta\omega\gamma_d\alpha^{-1}}{\gamma_d + \alpha_2\gamma\alpha^{-1}}$
Threshold (without noise)	$\gamma > 0$	$\gamma > \Delta\omega\gamma_d\alpha^{-1}$	$\gamma > \Delta\omega\gamma_d\alpha^{-1}$

Figure 9. Roots of the predator–prey system. This, from [9], gives the various roots of the multi-state predators–prey system. Note that both no-flow and finite-flow states are possible.

address realistic problems, such as the $L \rightarrow H$ and ITB transition, models with multiple predators, corresponding to zonal and mean shear flows, have been developed. Here, 'mean flows' refer to mean field $\langle \boldsymbol{E} \rangle \times \boldsymbol{B}$ shear flows, where the radial electric field $\langle E_r \rangle$ must satisfy the radial force balance equation. Thus, mean flows vary in space on profile scales. In contrast, zonal flows can occur on all mesoscales l, $\Delta_c < l < L_p$ where L_p is a profile scale length and Δ_c is the turbulence correlation length. Zonal flow spatial scales are set by those of the turbulence fluctuation intensity. The two predator-one prey model of Kim and Diamond [37], introduces such competition between mean and zonal shears, as well as a link between growth and mean shear on account of the *common* role of the pressure gradient in determining each. In this scenario, the zonal flow triggers the transition while the mean diamagnetic flow locks it in. Note that the concept of local gradient transport bifurcations builds upon the work of Itoh and Itoh [38], and Hinton [39]. The system evolution as predicted by these models is shown in figure 12. A slow power ramp reveals a period of dithering or limit cycle oscillations as the transition threshold is approached. During this period, turbulent fluctuations, zonal flows and ∇p all oscillate with a heat flux dependent relative phase. The competition between mean and zonal shears leaves a distinct signature upon the evolving wave form. In the fully evolved H-mode, turbulence is heavily suppressed. Thus, the zonal flow collapses, leaving only the mean flow to support the transport barrier. The multi-predator models [40] exhibit hysteresis (even in 0D!). Hysteresis is stronger in 1D models. Note that in these multi predator–prey models, the zonal flow controls access to the intermediate phase while the mean flow 'locks in' the H-phase.

Here, an interesting question arises, concerning the interplay of mean electric fields (n.b. we include neoclassical fields in the label 'mean') and zonal flows. The evolution of the sheared neoclassical electric field has been studied extensively [41] and recently has been included in full-f, global gyrokinetic simulations [42]. It is important to note that, as stated in [37], the mean and zonal electric shears are *not* simply additive, but instead have a rather complex network of feedback loops. In the multi-predator prey model:

(i) the pressure gradient can contribute to both prey and predator populations—the former via, say, ITG mode growth (i.e. $\gamma = \gamma(\nabla p)$) and the latter by its contribution to mean shears via radial force balance.

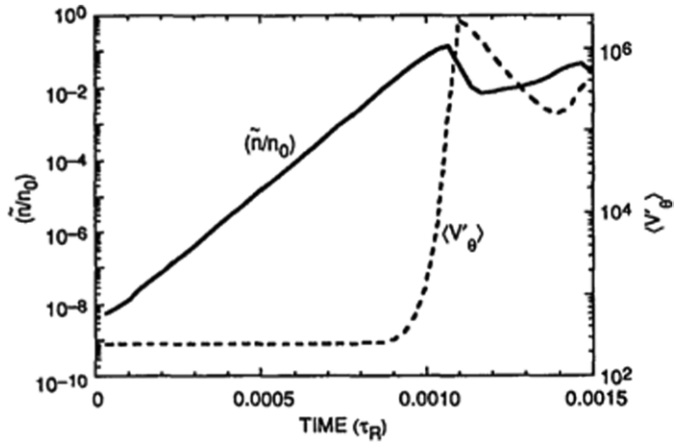

Figure 10. Time evolution of fluctuation intensity and turbulence driven flow from the simulation of [36]

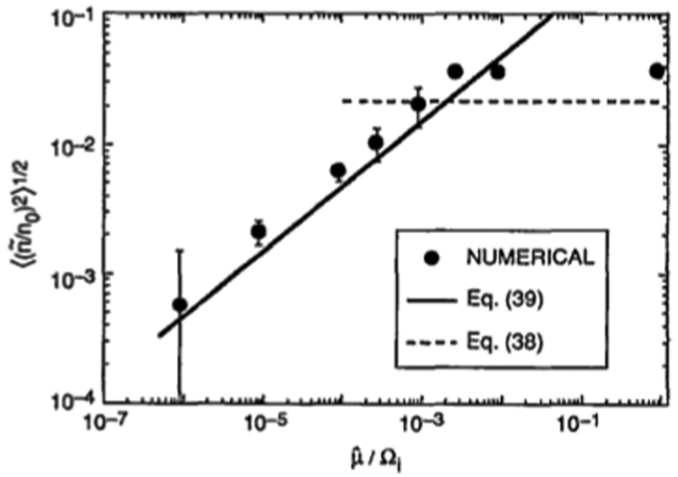

Figure 11. Fluctuation and flow damping. This, from a simulation of negative compressibility turbulence presented in [36], presents the scaling of the saturated fluctuation intensity ($\langle(\tilde{n}/n_0)^2\rangle$) with zonal flow damping μ. Note for small or moderate damping, the saturated intensity scales linearly with μ, as predicted by the predator–prey model. For strong damping, the zonal flow is effectively suppressed, so $\langle(\tilde{n}/n_0)^2\rangle$ becomes independent of μ.

(ii) mean field shear has a strong effect on the cross-phase of the fluctuation Reynolds stress $\langle\tilde{v}_r\tilde{v}_\theta\rangle$, which drives the zonal flow. As a consequence, mean field shear enters zonal flow dynamics *multiplicatively* and *nonlinearly*, so mean field shear can effectively reduce and/or cut off the generation of zonal flows by PV transport or inverse cascade. This is part of the L–H transition model proposed in [37].

(iii) zonal flows can, of course, enhance the growth of the mean shear by extracting fluctuation energy, thus reducing transport and so allowing ∇p to steepen, as discussed in [37].

(iv) the mean electric field directly enters the zonal flow dielectric [16, 43].

Indeed, the interaction of mean (neoclassical) and zonal shears is especially interesting in the context of stellerators, where purely neoclassical electric field bifurcations are possible and

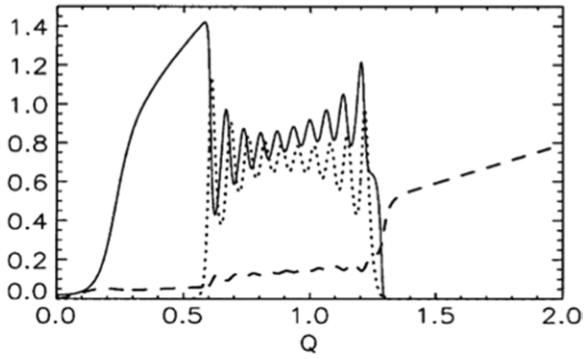

Figure 12. 2 predators and 1 prey. This figure, from [37], shows the evolution of the turbulence intensity, zonal flow intensity, and mean pressure gradient during a power ramp through an $L \to H$ transition. Here the solid line is the fluctuation (drift wave) intensity, the dotted line is the zonal flow intensity, and the dashed line is the mean pressure gradient. The x axis is normalized heat flux Q. Note that as heat flux Q increases, the system first enters a cyclic state, where fluctuation intensity and zonal flow intensity oscillate, while ∇p grows very slowly. At sufficient Q, turbulence and zonal flow collapse, and ∇p increases rapidly. This final state corresponds to an H-mode.

additional control parameters are available. All told, while the interaction of zonal and mean flows has been studied extensively, much work is still required for a complete understanding.

The basic ideas of zonal flow physics discussed here have been applied to numerous problems of current interest, which include but are not limited to: poloidal rotation [44], turbulence spreading [45, 46], confinement in plasmas with RMP [47, 48] and beta-plane MHD models of the solar tachocline [49, 50]. The interested reader is referred to the literature, as space does not permit even a short discussion of these, here. Rather we briefly discuss the current status of our understanding of flow shear dynamics in the $L \to H$ transition.

The $L \to H$ transition problem is singled out because since its discovery in 1982 [51], the $L \to H$ transition has driven much of the thinking and research on flows in magnetic fusion. In some sense, it has become *the* classic paradigm problem on flows in tokamaks. Also, the past two years have witnessed a remarkable spurt of progress in diagnosing flow and fluctuation behavior in edge plasmas at the transition threshold. In particular, studies by Conway *et al* on AUG [52], Estrada and Hidalgo [53, 54] on TJ-II, Schmitz [55] on DIII-D, McKee and Yan on DIII-D [56, 57], Kamiya and Ida [58] on JT-60U, Xu [59] on East, Hubbard [60] on Alcator C-Mod, and Zweben [61] on NSTX stand out as significant contributions. The gist of this wealth of information is that for $P \sim P_{\text{th}}$, limit cycle or dithering oscillations are observed in the flows and turbulence. These cyclic phenomena characterize what is now called the I-phase (I for intermediate, between L and H). Multi-shear flow competition is at work in the I-phase, and the flow structure evolves as the transition progresses. Many aspects of the observed phenomena are consistent with the multi-predator shearing model [37]. In particular, the variation of relative phases with increasing heat flux is observed. These are a variety of suggestions or hints as to the trigger mechanism. These include the GAM, zonal flow, mean $\boldsymbol{E} \times \boldsymbol{B}_0$ flow, mean poloidal flow and more. It is not at all obvious to these authors that there need be a unique route to the transition. Different shear flows may act as trigger under different circumstances. To face this challenge, theory should forsake the 0D models for one space-one-time-dimensional models of edge layer evolution. Theory should *predict* something qualitatively new. One suggestion as to where to look is the flow shear and fluctuation evolution during a slow, ELM free back-transition. Also, theory should link microdynamics to macroscopics, such as the

power threshold scalings. Both theory and experiment should elucidate SOL flow effects [62] on the shear structure *inside* the separatrix. This important issue remains terra incognita. Finally, basic experiments should be confronted to elucidate the details of the microscopic physical processes involved in shear layer formation [63]. Readers should stay tuned for excitement in the near future.

4. Inverse cascade and whistlerization of self-generated low frequency electromagnetic fluctuation: an extension of the Hasegawa–Mima equation

In this section, the nonlinear dynamics of electron magnetohydrodynamics (EMHD) is reviewed. EMHD plays an important role in space and magnetic confinement plasmas, in particular, in collisionless reconnection and in relativistic laser plasmas produced by an ultra intense short pulse laser, in particular, in the relativistic electron transport. In laser plasmas, magnetic fields are generated by the Weibel instability related to the relativistic electron transport which has been widely investigated in fast ignition research. In this section, the inverse cascade and the whistlerization in the Weibel turbulence are discussed in some detail.

4.1. Basic equations

The low frequency electromagnetic fluctuations (whistler turbulence) are generated by relativistic electron beams (electromagnetic two stream instability) and/or by anisotropy of electron momentum distribution (Weibel instability). When the scale length or the time scale of fluctuation is much shorter or faster than the ion scales, ions are assumed immobile and the incompressible electron fluid dynamics is taken into account. Namely, nonlinear dynamics of the fluctuation is described by the electron hydrodynamics (EMHD). The basic equations of EMHD are; The magnetic field induction equation:

$$\partial_t \boldsymbol{B} = -\nabla \times \boldsymbol{E}. \tag{31}$$

Electron fluid equation of motion:

$$\partial_t \boldsymbol{p} + \boldsymbol{v} \cdot \nabla \boldsymbol{p} = -e(\boldsymbol{E} + \boldsymbol{v} \times \boldsymbol{B}) - \frac{1}{n}\nabla P - \nu \boldsymbol{p}. \tag{32}$$

Ampere's law:

$$\frac{\nabla \times \boldsymbol{B}}{\mu} = \boldsymbol{j} = -en_0\boldsymbol{v} + \boldsymbol{j}_{\mathrm{ex}}. \tag{33}$$

Here, ions are immobile back ground and the electron fluid is assumed incompressible and the external current, $\boldsymbol{j}_{\mathrm{ex}}$ represents current carried by beam and/or high energy electron.

By introducing generalized vorticity, $\boldsymbol{\Omega} = \boldsymbol{\Omega}_B - \nabla \times \boldsymbol{v}$, equations (31) and (32) yield the vorticity equation;

$$\partial_t \boldsymbol{\Omega} - \nabla \times (\boldsymbol{v} \times \boldsymbol{\Omega}) = \nabla \times \left(\frac{\nabla P}{mn} + \nu_{\mathrm{e}} \boldsymbol{v} \right). \tag{34}$$

The right-hand side of equation (34) is the source (thermo electric effect) and dissipation of the vorticity. When the thermoelectric effects and the external current do not exist, equations (33) and (34) are combined to obtain a magnetic field evolution equation;

$$\partial_t \boldsymbol{\Omega} - \nabla \times (\boldsymbol{v} \times \boldsymbol{\Omega}) = \nabla \times \nu_{\mathrm{e}} \boldsymbol{v}, \tag{35}$$

$$\boldsymbol{\Omega} = \boldsymbol{\Omega}_B - \frac{c^2}{\omega_p^2} \nabla^2 \boldsymbol{\Omega}_B, \tag{36}$$

$$\boldsymbol{v} = -\frac{c^2}{\omega_p^2}\nabla \times \boldsymbol{\Omega}_B, \tag{37}$$

where $\boldsymbol{\Omega}_B = e\boldsymbol{B}/m$ is the electron cyclotron frequency. In equation (36), the second term is finite only when the magnetic fluctuation scale length is the order of electron skin depth. This is the electron Hall effect and the set of equations (35), (36) and (37) are the Hall EMHD equations. For the Weibel instability, beam instability or magnetic reconnection, the turbulence is essentially two-dimensional, like drift wave turbulence. In the two-dimensional turbulence, it is possible to introduce two scalar quantities, ψ and b and represent $\boldsymbol{\Omega}_B = e\boldsymbol{B}/m$ as

$$\boldsymbol{\Omega}_B = \hat{z} \times \nabla\psi + \hat{z}b. \tag{38}$$

Note that ψ is the magnetic flux function and the equi-contours of ψ represent magnetic field lines. The equations for ψ and b are obtained from equations (35), (36) and (37) by normalizing the space variables by the electron skin depth as follows:

$$\partial_t(\psi - \nabla^2\psi) + \hat{z} \times \nabla b \cdot \nabla(\psi - \nabla^2\psi) = \eta\nabla^2\psi, \tag{39}$$

$$\partial_t(b - \nabla^2 b) - \hat{z} \times \nabla b \cdot \nabla\nabla^2 b + \hat{z} \times \nabla\psi \cdot \nabla\nabla^2\psi = \eta\nabla^2 b. \tag{40}$$

Here, the right-hand side of equations (39) and (40) is the magnetic field dissipation due to resistivity. These equations are derived in [75]. It is known that the turbulence described by equations (39) and (40) exhibits inverse cascade or beam current filament merging. Note also that the first two terms of equation (40) are the same as the Hasegawa–Mima equation and the other nonlinear terms have a similar structure, namely, vector nonlinearity. From those characters of the equations, it is predicted that the inverse cascade occurs.

4.2. An example of nonlinear evolution of EMHD turbulence and self-organization in laser plasmas

The quasi-static magnetic field fluctuations are generated in relativistic laser plasmas. Figure 13(*a*) shows that an intense laser irradiates the over-dense from the left-hand side and relativistic electrons are generated and propagate from the left to right. Magnetic fields perpendicular to the simulation plane are generated and amplified. In figure 13(*b*), initially a relativistic beam is injected perpendicular to the simulation plane and temporal evolution of beam density distribution in the transverse plane is shown. This indicates that the electron beam break up into filaments and then they merged into few filaments. In the following, the merging process of electron beam filaments is discussed as the inverse cascade in the low frequency magnetic field turbulence. Figure 14 [68] shows self-generated magnetic filed temporal evolution, where the center of the initial beam is at the upper right corner. At the beginning, cylindrically symmetric magnetic field is generated due to the background electron shear flow.

Assuming the total vorticity of background electrons is conserved, then,

$$(\hat{z} \times \nabla(\psi - \nabla^2\psi))_\theta \sim \partial_r(\psi - \partial_r^2\psi) = A\delta(r - r_0). \tag{41}$$

The solution of equation (41) is easily obtained to show that the B field is localized and reversed at $r = r_0$ with the thickness of the order of the skin depth. This initial cylindrically symmetric magnetic field structure is consistent with figure 13(*a*). The cylindrical symmetry of the magnetic field is broken by the tearing instability.

Let us take a initial magnetic field as

$$\psi_0 = A\exp(\mathrm{i}k_0 x) + \text{c.c.} \tag{42}$$

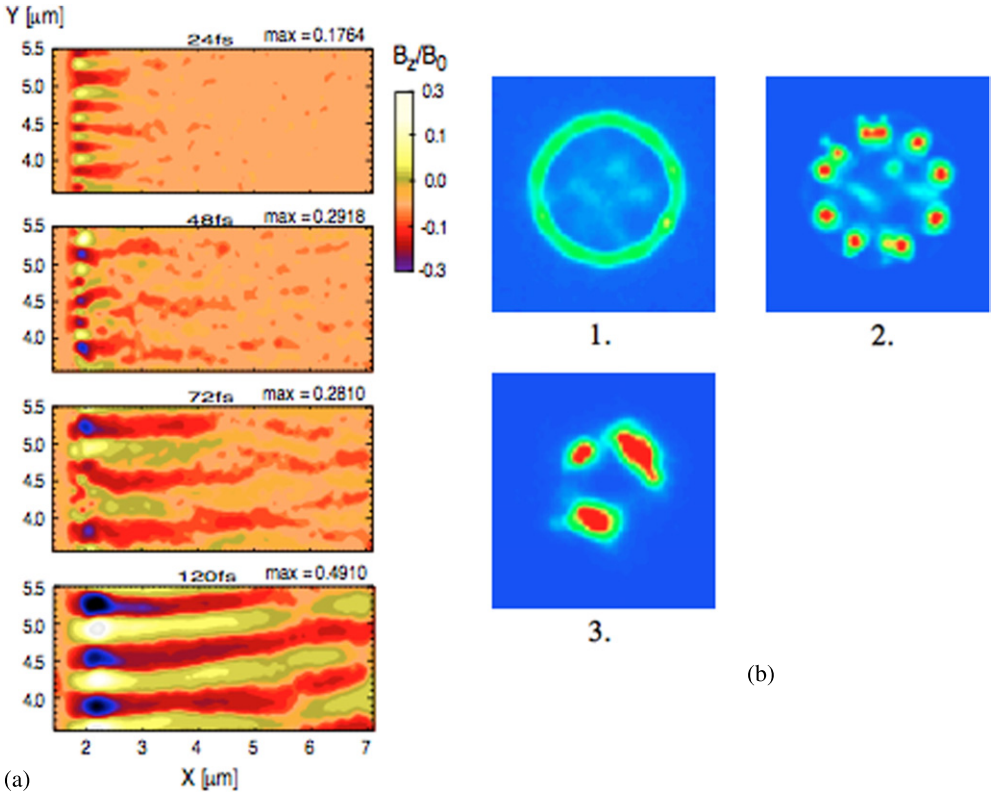

Figure 13. Quasi-static magnetic field generation by transverse two stream/Weibel instability by an intense electron beam. (*a*) 2D PIC simulation for the laser interaction with over dense plasma (5 times cut-off density). Magnetic field generation by the instability in laser produced plasmas, (*b*) 2D Hybrid simulation: particle (electron beam) and fluid (background plasma with the density of 10 times electron beam density). The electron beam density is shown in the figure. This figure indicates beam driven transverse two stream instability and merging of the electron beam.

and take perturbed magnetic fields as

$$\psi_1 = g\exp(\mathrm{i}ky) \qquad \text{and} \qquad b = h\exp(\mathrm{i}k_0 x + \mathrm{i}ky). \tag{43}$$

This mode structure is essentially the same as that of figure 13(*b*). The growth rate can be obtained by the linearized equation for ψ_1 and b;

$$\partial_t(\psi_1 - \nabla^2\psi_1) + \hat{z}\times\nabla b\cdot\nabla(\psi_0 - \nabla^2\psi_0) = 0, \tag{44}$$

$$\partial_t(b - \nabla^2 b) + \hat{z}\times\nabla\psi_1\cdot\nabla\nabla^2\psi_0 = 0. \tag{45}$$

The growth rate of this mode is given as follows:

$$\gamma(k) = B_0 k k_0 \left\{\frac{(1+k_0^2)(k_0^2-k^2)}{(1+k_0^2+k^2)(1+k^2)}\right\}^{1/2}. \tag{46}$$

This result indicates that both shorter and longer wavelength magnetic field fluctuations are simultaneously excited. The ratio of the energy of longer wavelength mode to that of the shorter wavelength mode is

$$\frac{(1+k^2)B_\perp^2}{(1+k_0^2+k^2)B_z^2} = \frac{k^2(1+k_0^2)}{k_0^2-k^2}. \tag{47}$$

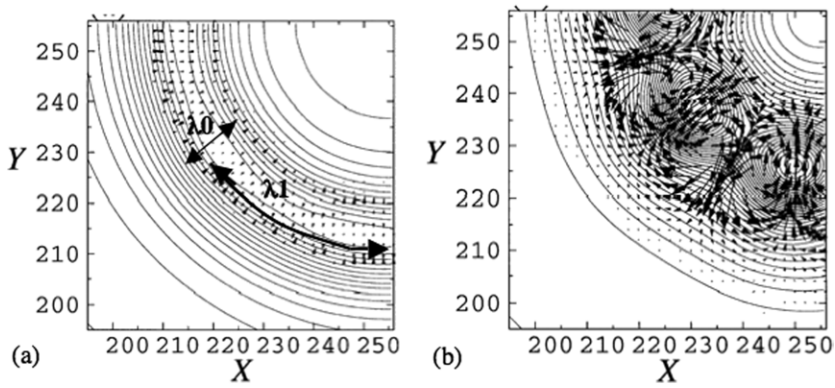

Figure 14. 2D Hybrid simulation where a relativistic electron beam propagates perpendicular to the X–Y plane. Temporal evolution of magnetic field lines excited by an electron beam (electron beam density is 10% of the back ground electron density) at $\omega_p t = 67$ and (*b*) $\omega_p t = 81$. The arrows in the figures show total electron fluxes.

This ratio is greater than unity for the maximum growing mode. This indicates that the inverse cascade of the two-dimensional EMHD is similar to the case of the Hasegawa–Mima equation [79]. The corresponding growth rate for the Hasegawa–Mima equation is

$$\gamma(k) = Ak^2 k_0 \left\{ \frac{k_0^2 - k^2}{(1 + k_0^2 + k^2)(1 + k^2)} \right\}^{1/2}. \tag{48}$$

In the simulation of [68], $k_0 > 1.0$, namely, the wavelength is comparable to the skin depth, c/ω_p, then the maximum growth rate is $\gamma(k) = 1.2\omega_c$ for $kc/\omega_p = 1.5$, $k_0 c/\omega_p = 3$. According to the simulation $\gamma \sim 0.24\omega_p$ for $\omega_c \sim 0.2\omega_p$.

After the long time inverse cascade, $k_0^2, k^2 \ll 1$ and $\gamma(k) \sim \omega_c (kc/\omega_p)^2$ is the time scale of long wave length whistler wave and $(B_z/B_\perp)^2$ will be 1 for the fastest growing mode according to equations (46) and (48). Figure 15 [68] shows that the nonlinear evolution of beam driven magnetic fluctuations can be reasonably described by the back ground electron nonlinearity, although high energy electron beams also respond to the magnetic field fluctuations.

As the final state, it is expected that magnetic bubbles of the helical structure are formed in the two-dimensional EMHD turbulence. Equations (39) and (40) have three conserved quantities, which are energy, magnetic flux and cross helicity as derived by Das *et al* [75]. Minimizing the energy for a fixed flux and cross helicity, an attractor of magnetic structure evolution can be obtained. It will be a helical structure with $\langle B_z \rangle^2 = \langle B_\perp \rangle^2$. Further analysis will be continued in future studies.

5. Conclusion

As to conclusions, there are none. This topic is alive and well, and will evolve dynamically. The cross-disciplinary dialogue with the geophysical and astrophysical fluids has surely been beneficial and should continue. Indeed, we still have much to learn. As theorists should *predict*, rather than merely explain, here we predict that this will not be the last prize awarded for the theory of drift wave–zonal flow turbulence.

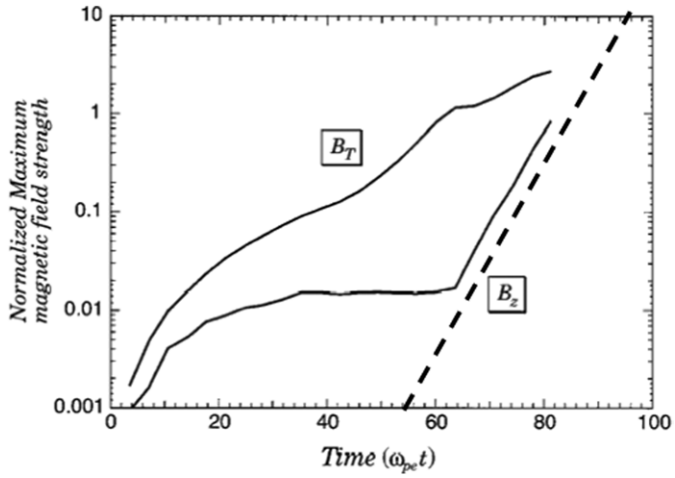

Figure 15. Maximum magnetic field strength in the simulation region. Here, B_T is the transverse component to the beam propagation, and B_z is the parallel components to it.

Acknowledgments

The authors would like to express their gratitude to the European Physical Society for providing the opportunity of submitting this paper in connection with the Alfven Prize award. Hasegawa is grateful to the late Professor Toshiya Taniuti who guided him to the realm of nonlinear physics, in particular to soliton and vortex dynamics. He is indebted to the late Professor Masahiro Wakatani who provided him with continued opportunities to work together in Kyoto and performed critical computer simulations of turbulent plasmas. Hasegawa is also grateful to Professor Zhihong Lin for valuable discussions and for providing him with critical simulation results related to zonal flow generations.

One of the authors (PHD) acknowledges the superb scientific and human mentorship by the late Marshall N Rosenbluth. PHD thanks Thomas H Dupree, B A Carreras, Sanae-I Itoh, Kimitaka Itoh, Taik Soo Hahm and Ozgur Gurcan for their valuable contributions to these ideas and work at various points in his career. PHD also thanks many other theoretical and experimental colleagues and co-workers for their contributions. This work was supported by the United States DOE and the Korean NRFWCI Program. Finally, PHD adds that from 2001 to the present, the biannual Festival de Theorie, organized by the CEA of France, has been a valuable sources of scientific stimuli.

All the authors thank Yusuke Kosuga for valuable assistance with the preparation of this manuscript.

References

[1] Slusher R E and Surko C M 1976 *Phys. Rev. Lett.* **37** 1747
[2] Mazzucato E 1976 *Phys. Rev. Lett.* **37** 792
[3] Slusher R E and Surko C M 1978 *Phys. Rev. Lett.* **40** 400
[4] Kraichnan R H 1973 *J. Fluid Mech.* **59** 745
[5] Hasegawa A and Mima K 1978 *Phys. Fluids* **21** 1
[6] Onsager L 1949 *Nuovo Cimento (suppl)* **6** 279
[7] Kolmogorov A N 1941 *Dokl. Akad. Nauk SSR* **30** 301
[8] Hasegawa A and Wakatani M 1983 *Phys. Rev. Lett.* **50** 682

[9] Diamond P H, Itoh S-I, Itoh K and Hahm T S 2005 *Plasma Phys. Control. Fusion* **47** R35
[10] Sagdeev R Z, Shapiro V D and Shevchenko V I 1978 *Sov. J. Plasma Phys.* **4** 306
[11] Hasegawa A, Maclennan C G and Kodama Y 1979 *Phys. Fluids* **22** 2122
[12] Hasegawa A and Wakatani M 1987 *Phys. Rev. Lett.* **59** 1581
[13] Carreras B A, Lynch V E and Garcia L 1991 *Phys. Fluids* B **3** 1438
[14] Waltz R E, Kerbel G D and Milovich J 1994 *Phys. Plasmas* **1** 2229
[15] Xiao Y, Holad I, Zhang W, Klasky S and Lin Z 2010 *Phys. Plasmas* **17** 022302
[16] Rosenbluth M N and Hinton F L 1998 *Phys. Rev. Lett.* **80** 724
[17] Champeaux S and Diamond P H 2001 *Phys. Lett.* A **288** 214
[18] Taniuti T and Yajima N 1969 *J. Math. Phys.* **10** 1369
[19] Nozaki K, Taniuti T and Watanabe K 1979 *J. Phys. Soc. Japan* **46** 983
[20] Nozaki K, Taniuti T and Watanabe K 1979 *J. Phys. Soc. Japan* **46** 991
[21] Andrews D G and McIntyre M E 1978 *J. Fluid Mech.* **89** 647
[22] Charney J G 1948 *Geof. Publ.* **17** 3
[23] Charney J G and Drazin P G 1961 *J. Geophys. Res.* **66** 83
[24] Taylor G I 1915 *Phil. Trans. R. Soc. Lond.* **A215** 1
[25] Diamond P H and Kim Y B 1991 *Phys. Fluids* B **3** 1626
[26] Diamond P H *et al* 1993 *Plasma Physics Controlled Nuclear Fusion Research 1992* vol 2 (IAEA: Vienna)
[27] Tobias S M, Dagon K and Marston J B 2011 *Astrophys. J.* **727** 127
[28] Diamond P H, Gurcan O D, Hahm T S, Miki K, Kosuga Y and Garbet X 2008 *Plasma Phys. Control. Fusion* **50** 124018
[29] Dupree T H 1966 *Phys. Fluids* **9** 1773
[30] Biglari H, Diamond P H and Terry P W 1990 *Phys. Fluids* B **2** 1
[31] Hahm T S and Burrell K H 1995 *Phys. Plasmas* **2** 1648
[32] Carreras B A, Sidikman K, Diamond P H, Terry P W and Garcia L 1992 *Phys. Fluids* B **4** 3115
[33] Diamond P H *et al* 2001 *Nucl. Fusion* **41** 1067
[34] Chen L, Lin Z and White R 2000 *Phys. Plasmas* **7** 3129
[35] Diamond P H, Liang Y-M, Carreras B A and Terry P W 1994 *Phys. Rev. Lett.* **72** 2565
[36] Charlton L A, Carreras B A, Lynch V E, Sidikman K L and Diamond P H 1994 *Phys. Plasmas* **1** 2700
[37] Kim E-J and Diamond P H 2003 *Phys. Rev. Lett.* **90** 185006
[38] S-I-Itoh and Itoh K 1988 *Phys. Rev. Lett.* **60** 2276
[39] Hinton F L 1991 *Phys. Fluids* B **3** 696
[40] Malkov M A and Diamond P H 2009 *Phys. Plasmas* **16** 012504
[41] Rozhansky V and Tendler M 1992 *Phys. Fluids* B **4** 1877
[42] Chang C S, Ku S, Diamond P H, Lin Z, Parker S, Hahm T S and Samatova N 2009 *Phys. Plasmas* **16** 056108
[43] Sugama H and Watanabe T-H 2006 *Phys. Plasmas* **13** 012501
[44] McDevitt C J, Diamond P H, Gurcan O D and Hahm T S 2010 *Phys. Plasmas* **17** 112509
[45] Gurcan O D, Diamond P H, Hahm T S and Lin Z 2005 *Phys. Plasmas* **12** 032303
[46] Gurcan O D, Diamond P H and Hahm T S 2006 *Phys. Plasmas* **13** 052306
[47] Leconte M and Diamond P H 2011 *Phys. Plasmas* **18** 082309
[48] Xu Y *et al* 2011 *Nucl. Fusion* **51** 063020
[49] Hughes D W, Rosner R and Weiss N O 2007 *The Solar Tachocline* (Cambridge: Cambridge University Press)
[50] Tobias S M, Hughes D W and Diamond P H 2007 *Astrophys. J.* **667** L113
[51] Wagner F *et al* 1982 *Phys. Rev. Lett.* **49** 1408
[52] Conway G D *et al* 2011 *Phys. Rev. Lett.* **106** 065001
[53] Estrada T *et al* 2009 *Plasma Phys. Control. Fusion* **51** 124015
[54] Estrada T *et al* 2010 *Euro. Phys. Lett.* **92** 35001
[55] Schmitz L *et al* 2011 *Phys. Rev. Lett.* submitted
[56] McKee G R *et al* 2001 *Nucl. Fusion* **41** 1235
[57] Yan Z *et al* 2011 *Phys. Plasmas* **18** 056117
[58] Kamiya K *et al* 2010 *Phys. Rev. Lett.* **105** 045004
[59] Xu G S *et al* 2011 *Phys. Rev. Lett.* **107** 125001
[60] Hubbard A E *et al* 2011 *Phys. Plasmas* **18** 056115
[61] Zweben S J *et al* 2010 *Phys. Plasmas* **17** 102502
[62] LaBombard B *et al* 2004 *Nucl. Fusion* **44** 1047
[63] Xu M *et al* 2011 *Phys. Rev. Lett.* **107** 055003
[64] Kingsep A S, Chukbar K V and Yankov V V 1990 *Reviews of Plasma Physics* vol 16 (New York: Consultant Bureau)

Kingsep A S, Chukbar K V and Yankov V V 1982 *Reviews of Plasma Physics* p 1408
[65] Honda M, Myer-ter-Vehn J and Pukov A 2000 *Phys. Plasmas* **7** 1302
[66] Honda M, Myer-ter-Vehn J and Pukov A 2000 *Phys. Rev. Lett.* **85** 2128
[67] Sentoku Y, Mima K, Kaw P K and Nishikawa K 2003 *Phys. Rev. Lett.* **90** 155001
[68] Taguchi T, Anonsen T M Jr, Liu C S and Mima K 2001 *Phys. Rev. Lett.* **86** 5055 submitted
[69] Cai H B, Zhu S P, Chen M, Wu S, He X T and Mima K 2011 *Phys. Rev.* E **83** 036408
[70] Sentoku Y, Mima K, Kojima S and Ruhl H 2000 *Phys. Plasmas* **7** 689
[71] Bulanov S V, Pegoraro F and Sakharov A S 1992 *Phys. Fluids* B **4** 2499
[72] Drake J F, Kleva R G and Mandt M E 1994 *Phys. Rev. Lett.* **73** 1251
[73] Biskamp D 1997 *Phys. Plasmas* **4** 1964
[74] Biskamp D, Schwarz E and Drake J F 1996 *Phys. Rev. Lett.* **76** 1264
[75] Mandt M E, Denton R E and Drake J F 1994 *Geophys. Res. Lett.* **21** 73
[76] Das A and Diamond P H 2000 *Phys. Plasmas* **7** 170
[77] Lukin V S 2009 *Phys. Plasmas* **16** 122105
[78] Fonseca R A *et al* 2003 *Phys. Plasmas* **10** 1979
[79] Nishikawa K-I, Hardee P, Richardson G, Preece R, Sol H and Fishman G J 2005 *Astrophys. J.* **622** 927
[80] Hasegawa A and Kodama Y 1978 *Phys. Rev. Lett.* **41** 1470